THE JOURNAL OF BIOLOGICAL CHEMISTRY VOL. 283, NO. 8, pp. 4730–4743, February 22, 2008

Proteomic Analysis of a Nutritional Shift-up in *Saccharomyces cerevisiae* Identifies Gvp36 as a BAR-containing Protein Involved in Vesicular Traffic and Nutritional Adaptation*[S]

Received for publication, September 17, 2007, and in revised form, December 21, 2007 Published, JBC Papers in Press, December 21, 2007, DOI 10.1074/jbc.M707787200

Lorenzo Querin[‡1,2], **Rossella Sanvito**[§1,3], **Fulvio Magni**[§], **Stefano Busti**[‡], **Alain Van Dorsselaer**[¶], **Lilia Alberghina**[‡], **and Marco Vanoni**[1,4]

From the [‡]*Department of Biotechnology and Biosciences, University Milano-Bicocca, 20126 Milano, Italy, the* [§]*University Milano-Bicocca, DIMESAB, 20052 Monza, Italy, and the* [¶]*CNRS, University Louis Pasteur, LSMBO, F-67070 Strasbourg, France*

Yeast cells undergoing a nutritional shift-up from a poor to a rich carbon source take several hours to adapt to the novel, richer carbon source. The budding index is a physiologically relevant "global" parameter that reflects the complex links between cell growth and division that are both coordinately and deeply affected by nutritional conditions. We used changes in budding index as a guide to choose appropriate, relevant time points during an ethanol to glucose nutritional shift-up for preparation of samples for the analysis of proteome by two-dimensional electrophoresis/mass spectrometry. About 600 spots were detected. 90 spots, mostly comprising proteins involved in intermediary metabolism, protein synthesis, and response to stress, showed differential expression after glucose addition. Among modulated proteins we identified a protein of previously unknown function, Gvp36, showing a transitory increase corresponding to the drop of the fraction of budded cells. A *gvp36*Δ strain shares several phenotypes (including general growth defects, heat shock, and high salt sensitivity, defects in polarization of the actin cytoskeleton, in endocytosis and in vacuolar biogenesis, defects in entering stationary phase upon nutrient starvation) with secretory pathway mutants and with mutants in genes encoding the two previously known yeast BAR proteins (*RSV161* and *RSV167*). We thus propose that Gvp36 represents a novel yeast BAR protein involved in vesicular traffic and in nutritional adaptation.

Although glucose represents its favored substrate, the budding yeast *Saccharomyces cerevisiae* can utilize a wide range of fermentable and non-fermentable carbon sources. Pathways for the assimilation of alternative carbon sources are repressed in the presence of glucose that also activates glycolysis, decreases respiratory activity, increases ribosome biogenesis, and regulates growth and development through alteration in gene expression, post-transcriptional and translational regulation. For instance, a large number of yeast genes, including those required for galactose utilization, the tricarboxylic acid cycle, and gluconeogenic genes are transcriptionally repressed by glucose (1–3), whereas transcription of genes encoding glycolytic enzymes, hexose transporters, and ribosomal proteins is transcriptionally activated by glucose (3–8). A few yeast mRNAs, including the *SDH2*, *SUC2*, *SPO13*, *PCK1*, and *FBP1* mRNAs have been reported to be post-transcriptionally regulated by glucose (9–12). Moreover, integrated genomic and proteomic approaches to investigate the effects of carbon source on gene expression in *S. cerevisiae*, exponentially growing on either fermentable and non-fermentable carbon source, have shown that in many cases mRNA abundance is not a reliable indicator of corresponding protein abundance (13, 14), suggesting that other mechanisms in addition to transcriptional control may be very important for adaptation to nutrients.

In the wild, sudden transitions from one carbon source to another, as well as from conditions of large food supply to its disappearance, represent the rule and not the exception (15). Thus, yeast has evolved a wide array of signal transduction pathways, coordinating the various metabolic, developmental, and cellular response pathways to carbon source availability.

When inoculated into a medium rich in glucose, *S. cerevisiae* can convert glucose to ethanol by "fermentation", the preferred method of yeast metabolism. Yeast utilizes other energy/carbon sources only after glucose exhaustion. The preferred energy/carbon source after glucose is exhausted is ethanol, which is available in high concentrations at that point. The shift from anaerobic fermentation of glucose to aerobic respiration of ethanol is called the "diauxic shift" and is known to be accompanied by major changes in gene expression (1), not surprising because entire metabolic pathways need to be activated or deactivated.

A wide variety of enzymes are induced during the diauxic shift. These include enzymes involved in gluconeogenesis, the glyoxylate cycle, the tricarboxylic acid cycle, and respiration (16, 17). Proteomics (18–20) highlighted that three major events take place during the diauxic shift: (i) an induction of

* This work was supported by grants from Ministero dell'Universitá e della Ricerca (MIUR) (Fondo per le Agevolazioni alla Ricerca and COFIN2006) (to M. V.) and MIUR (Fondo per gli Investimenti della Ricerca di Base-ITALBionet) (to L. A.). The costs of publication of this article were defrayed in part by the payment of page charges. This article must therefore be hereby marked "*advertisement*" in accordance with 18 U.S.C. Section 1734 solely to indicate this fact.

[S] The on-line version of this article (available at http://www.jbc.org) contains supplemental Figs. S1–S8 and Tables S1–S4.

[1] Contributed equally to this work.

[2] Present address: DiaSorin S.p.A., c/o Nerviano Medical Science, Viale Pasteur 10, 20014 Nerviano, Italy.

[3] Present address: Merck Serono S.p.A., Structural Characterization Lab., Via Valle Caia 22, 00040 Ardea, Italy.

[4] To whom correspondence should be addressed: Piazza della Scienza 2, 20126 Milano, Tel.: 39-02-64483525; Fax: 39-02-64483519; E-mail: marco.vanoni@unimib.it.

proteins involved in the general stress response; (ii) the induction of glucose-repressed proteins; and (iii) a transient arrest in the synthesis of proteins present in exponentially growing cells. Genome-wide transcriptional analysis also identified distinguishable functional clusters of genes that are co-regulated when glucose becomes limiting (1). Proteomic analysis has also been later extended to mutants in genes within the Snf1 kinase pathway, a major regulatory pathway involved in sensing of intracellular glucose and/or energy charge in yeast (21).

The reverse shift is the so-called ethanol-glucose nutritional shift-up, where cells growing on media supplemented with ethanol as a sole carbon source are fed with glucose. The pattern of macromolecular syntheses, cell mass increase, and budding dynamics defining major phases during the shift-up are schematically reported in Fig. 1, which summarizes many published results (22, 23). In ethanol-supplemented media, cells grow slower and are smaller. Soon after addition of glucose, overall increase in mass, detected by turbidometry, decreases dramatically for the first 2 h after the shift-up. Incorporation of radioactive precursors suggested that, in keeping with what was observed in other eukaryotic microorganisms (24), the rate of RNA synthesis is stimulated before the rate of protein synthesis, both ultimately reaching the higher value, characteristic of the novel steady state condition (22). The change in protein biosynthetic capacity brought about by increased ribosome content needs to be coordinated with cell cycle and cell division. Because G_1 cells in yeast correspond approximately to unbudded cells, the budding index, *i.e.* the fraction of budded cells in the population, represents a sensitive physiological parameter that can be used to easily monitor population dynamics during the shift-up. During the first part of the shift-up, two major delays are observed: cells that were in G_1 at the moment of the shift delay their entry into S phase, whereas cells that had already executed the G_1 to S transition delay completion of the cell cycle (23, 25). Accordingly, the shift-up events can be dissected in different phases, all convergent to allow a rapid transition to cells growing faster, with a higher protein content at the G_1 to S transition and a shorter budding time compared with pre-shift cells.

Among the ~600 spots detected by two-dimensional PAGE, 90 spots (plus 48 that we mark as "potentially changed" because they did not pass the most rigid criteria for significance), mostly comprising proteins involved in intermediary metabolism, protein synthesis, and response to stress, showed differential expression after glucose addition. Among modulated proteins we identified a protein of previously unknown function, Gvp36,[5] which shows a transitory increase corresponding to the drop of the fraction of budded cells. Based on bioinformatic, genetic, and biochemical analysis, we propose Gvp36 as a novel yeast BAR protein involved in vesicular traffic and in nutritional adaptation. Phenotypes of *gvp36*Δ mutants, including general growth defects, heat shock sensitivity, and poor growth at 37 °C, sensitivity to high salt, defects in polarization of the actin cytoskeleton, in endocytosis and vacuolar biogenesis, and defects in nutritional adaptation are compatible with known BAR domain functions in binding and/or bending cellular membranes.

EXPERIMENTAL PROCEDURES

Strains and Vectors—The *S. cerevisiae* haploid strain used in this study is *W303-1A* (*Mata, ade2-1, leu2-3, ura3-1, trp1-1, his3-11*) or its *W303-CF* derivative. In *W303-CF*, both Cln3 and Far1 proteins are tagged with a 15-Myc tag. The strain is phenotypically indistinguishable from the parent strain in a variety of growth conditions on the basis of duplication time, fraction of budded cells, average protein content, and overall morphology (26).

Deletion of *GVP36* was performed with transformation and homologous recombination of standard auxotrophic deletion cassettes. Yeast cell transformations were performed according to standard lithium acetate method. *gvp36*Δ mutant was compared with the *W303-1A* wild type strain. The *GVP36-TAP* tagged strain (*MAT***a** *his3*Δ*1 leu2*Δ*0 met15*Δ*0 ura3*Δ*0 GVP36-TAP*) (27) was purchased from Open Biosystems.

Growth Conditions—Yeast cells were grown at 30 °C in synthetic complete (SC) medium (Bio 101 Inc.) with yeast nitrogen base (Difco) as a nitrogen source, or in YPD medium (1% yeast extract, 2% peptone), supplemented with 2% glucose (SCD-YPD), 2% ethanol (SCE), or 3% glycerol (SCG-YPG) as carbon source, or in minimal medium (YNB) containing yeast nitrogen base and (per liter) 5 mg of adenine, 5 mg of uracil, 5 mg of leucine, 5 mg of histidine, 5 mg of tryptophan, and supplemented with 2% glucose (YNBD). For nitrogen starvation, we used a minimal medium supplemented with yeast nitrogen base without ammonium sulfate and with 3% glycerol as carbon source (YNBG).

To examine growth of yeast strains in different carbon source containing media, serially diluted cells were spotted (5 μl) on solid YP or SC medium supplemented with 2% glucose, 2% ethanol, or 3% glycerol, or on solid YNB medium supplemented with 0.05, 0.1, 0.25, or 0.5% glucose. To test ethanol sensitivity and osmosensitivity, exponentially growing in YPD cells were serially diluted and spotted onto YPD solid medium either 2 or 4% ethanol, and onto YPD solid medium supplemented with different sorbitol concentrations. To test salt sensitivity, cells exponentially growing in YPD cells were serially diluted and either spotted or plated (to assessed their viability) onto YPD or YNBD solid medium supplemented with 6% NaCl or 6% $MgCl_2$. To test thermosensitivity for growth, cells exponentially growing in YPD cells were serially diluted and plated onto YPD or YNBD solid medium, supplemented or not supplemented with 1 M sorbitol, and then incubated at 30 or 37 °C: their viability was assessed by counting colony forming units. Finally, to test heat shock resistance, confluence grown cells (about $1–2 \times 10^8$ cells/ml, grown 2 or 7 days in YPD medium) were treated at 51 °C for 5, 10, 15, or 20 min and then plated onto YPD solid medium: their viability was assessed by counting colony forming units.

[5] The abbreviations used are: Gvp36, Golgi vesicle protein of 36 kDa; Lat-B, latrunculin-B; BI, budded index; YNB, yeast nitrogen base; SSD, steady state in dextrose; LY, Lucifer yellow; MALDI-TOF, matrix-assisted laser desorption ionization time-of-flight; LC-MS/MS, liquid chromatography-tandem mass spectrometric; PBS, phosphate-buffered saline; CHAPS, 3-[(3-cholamidopropyl)dimethylammonio]-1-propanesulfonic acid; CDCFDA, [5-(and -6)-Carboxy-2′,7′-dichlorofluorescein diacetate].

To study nutritional shift-up, at time 0 2% glucose was added to cells exponentially growing in ethanol or glycerol-supplemented medium and samples were collected to evaluate the percentage of budded cells; for proteomic analyses cells were collected at the times indicated in Fig. 1; a control yeast population exponentially growing on 2% glucose was also collected.

For α-factor block-and-release experiments, cells were grown to exponential phase at 25 °C in YPD medium and α-factor was added to a final concentration of 2.5 μg/ml. After 120 min of α-factor treatment cells were filtered, washed with 3 volumes of YP medium without glucose, and resuspended in fresh YPD medium containing 15 μg/ml nocodazole. After 150 min, when most of the cells had a very large bud, cells were filtered, washed with 5 volumes of YP medium without glucose, and resuspended in fresh YPD medium containing 2.5 μg/ml α-factor.

Latrunculin-B Treatment—Sensitivity to Lat-B was performed essentially as previously described (28). Briefly, cells exponentially growing in YPD (10^5 cells) were plated onto YPD solid medium. Lat-B was diluted into Me_2SO and 4 μl of vehicle or the indicated concentration of Lat-B were pipetted onto a 6-mm filter disk (Schleicher and Schuell), which was placed onto the top agar. Plates were placed at 30 °C for 24–48 h.

Cell Cycle and Growth Parameters—Cells were counted after sonication with a Coulter Counter Z2. The specific growth rate (μ) was assessed by fitting the cell number against time and duplication time (Td) calculated subsequently according to equation $Td = \ln 2/\mu$. The fraction of total budded cells (Fb) was calculated after microscopic examination (at least 300 cells per count were scored).

Cytofluorimetric Analysis—Determination of protein and DNA contents was performed on cells fixed in 70% ethanol (v/v) as previously described (26). Total proteins were stained with fluorescein isothiocianate and total DNA with Sytox® Green (Molecular Probes). Analysis was performed with a FACScan (BD Biosciences) equipped with a Ion-Argon laser at 488 nm laser emission.

Fluorescence Microscopy—Fluorescence microscopy was carried out with a Nikon Eclipse E600 microscope. Images were captured with LEICA DC350F camera controlled by Leica FW4000 software.

Actin Localization—Cells were fixed by addition of formaldehyde to a final concentration of 3.7%. After 1 h, cells were collected by centrifugation, washed twice in phosphate-buffered saline (PBS) (127 mM NaCl, 6.7 mM Na_2HPO_4, 3.3 mM NaH_2PO_4, 0.2 mM EDTA, adjusted to pH 7.5), resuspended in 25 μl of PBS containing 2 ng/μl of rhodamine-conjugated phalloidin (Molecular Probes) (from a stock solution of 100 ng/μl in methanol). After 3 h at 25 °C, cells were washed five times with PBS and mounted directly for fluorescence microscopy observation.

Classification of Cells Depending on Actin Polarization State—Approximately 100 small- and medium-budded cells, exponentially grown in YPD medium, were scored as having: >90% of their actin in the bud (polarized cells); 50–90% of their actin in the bud (partially depolarized cells); or <50% of their actin in the bud (totally depolarized cells).

Vacuole Staining—For FM4-64 (Molecular Probes) staining, cells exponentially grown in SCD medium were harvested and resuspended in the same medium. FM4-64 was added to 80 μM from a stock solution of 4 mM Me_2SO. Cells were then incubated with shaking for 60 min at 30 °C. After this preliminary labeling step, cells were harvested, resuspended in fresh SCD medium, and incubated with shaking for 3 h at 30 °C. After a single wash with PBS, cells were placed on standard slides and observed. For CDCFDA (Molecular Probes) staining, cells exponentially grown in SCD medium were harvested and resuspended in the same medium containing 500 μM CDCFDA (added from a 100 mM stock solution in Me_2SO). Cells were then incubated with shaking for 30–45 min at 30 °C. Finally, cells were washed three times with PBS and viewed. For Lucifer yellow (LY) accumulation experiments, cells exponentially grown in SCD medium were harvested and resuspended in the same medium, added with 10 mg/ml LY (Sigma). Cells were then incubated with shaking for 3 h at 30 °C in dark. After washing four times with ice-cold 50 mM sodium succinate buffer, pH 5, containing 20 mM sodium azide, cells were resuspended in the same buffer and viewed.

Protein Extraction—Typically, 1×10^9 cells/sample were collected by filtration, washed twice with cold water, and immediately frozen at −80 °C. Samples were slowly thawed on ice. Cells were resuspended in lysis buffer (0.1 M Tris-HCl, pH 7.5, 1 mM EDTA) plus proteases inhibitor mixture (Complete EDTA-free Protease Inhibitor Mixture Tablets, Roche) and 1 mM phenylmethylsulfonyl fluoride. An equal volume of acid-washed glass beads (Sigma) were added, and cells were broken by 10 vortex/ice cycles of 1 min each on ice. Extracts were transferred in new tubes and clarified by centrifugation. Protein concentration was determined using the Bio-Rad protein assay.

Evaluation of Gvp36-TAP Expression Levels—Cultures of the Gvp36-TAP tagged strain were subjected to a nutritional shift-up and cellular samples (3×10^8 cells) were collected at regular intervals to evaluate the expression of the tagged protein. Protein extracts were prepared as described above. Rabbit anti-TAP antibodies (Open Biosystems) were used for Western blot analysis. Densitometric analysis of the bands corresponding to the tagged protein was performed using the ImageJ software.

Two-dimensional PAGE—250 μg of proteins were desalted with Micro Bio-Spin Chromatography Columns Bio-Gel P-6 (Bio-Rad), dried, and then resuspended in 300 μl of a solution containing urea (7 M), thiourea (2 M), CHAPS (4% w/v), Tris (40 mM), dithioerythritol (65 mM), Resolyte pH 3–10 (0.5% v/v), and a trace of bromphenol blue. The whole yeast-diluted sample was loaded onto the IPG gel strip (pH 3–10 nonlinear, 17 cm, Bio-Rad). Hydration was performed overnight at 50 V and 20 °C in the PROTEAN IEF Cell (Bio-Rad). In the first dimension, proteins were separated using a gel containing a non-linear immobilized pH gradient (200 V for 1 h; increase to 1000 during 1 h, then to 4000 during 45 min; 4000 V for 3 h; increase to 8000 V during 1 h and 30 min; 8000 V for 3 h). The strips were equilibrated with a solution containing 0.05 M Tris-HCl, pH 6.8, 6 M urea, 30% (v/v) glycerol, 2% (w/v) SDS, and 2% (w/v) dithioerythritol for 15 min, and subsequently another 15 min with the same solution with 2.5% (w/v) iodoacetamide instead of dithio-

erythritol. Second dimension was performed in polyacrylamide gradient gels (7.5–16%) with the Ettan DALTsix electrophoresis unit (Amersham Biosciences) at 20 mA per gel at 8 °C. The gels were stained overnight with GelCode® (Pierce).

The shift-up experiment was performed in triplicate. To assure a good comparison, for each experiment six gels were run simultaneously at the first and second dimensions.

Image Capture and Analysis—Image scanning was performed on a Bio-Rad GS-800 calibrated imaging densitometer and the spots analyzed using PDQuest 7.1.1 (Bio-Rad). Normalization of spot volumes in gel was performed using the "total density in valid spots" option. For each protein spot, normalized spot quantity from the gel taken at t_0 (supplemental Table S3) was used as a reference: the relative expression level at each later time point (*i.e.* t_1, t_2, t_3, t_4, and steady state in dextrose (SSD)) was calculated by dividing the normalized spot quantity in each gel by the level of the t_0 reference gel. Three independent shift-up experiments were run (biological triplicate). We considered as "changed" proteins whose relative expression levels varied at least 1.5-fold in all three biological replicates. Spots showing verified changes only in two of three gels were classified as "potentially changed." In the case of Gvp36, additional experiments using a different technique allowed to confirmation of reproducibility, moving the protein from the potentially changed to the changed class. Analysis of time-dependent changes in relative expression levels provides a further internal control, because it seems unlikely that a spot showing variations in its intensity at multiple time points can be erroneously classified as changed. Consistently, among the 90 spots designed as changed by the above criteria, only 3 showed altered expression at a single time point. Moreover, about 90% of spots designed as changed fell into a limited number of pathways, about 60% being involved in intermediary metabolism. Taken together these findings indicate that the use of a low threshold value did not result in an excessive number of spots erroneously classified as changed.

Clustering—*K*-means clustering was performed on data obtained from bidimensional electrophoresis using the Pearson Correlation by J-Express pro 2.7 (see molmine.com for program details).

In Gel Digestion—*In situ* digestion of the gel spots was performed with an automated protein digestion system, MassPREP Station (Waters) (29). The gel plugs were washed three times with a mixture of 1:1 25 mM NH_4HCO_3/ACN. The cysteine residues were reduced with dithiothreitol at 57 °C (10 mM in 25 mM NH_4HCO_3, 1 h) and alkylated with iodoacetamide (25 mM in 25 mM NH_4HCO_3, 45 min). After dehydration with ACN, the proteins were digested in-gel with modified porcine trypsin (Promega, Madison, WI; 10 μl of 12.5 ng/μl in 25 mM NH_4HCO_3) overnight at 37 °C. The volume of trypsin added was estimated visually according to the piece of gel size (4–6 μl).

Peptide Extraction—MALDI-TOF analysis was carried out on tryptic peptides extracted with 4 μl of 35% H_2O, 60% ACN, 5% HCOOH (v/v/v). For nanoscale capillary liquid chromatography-tandem mass spectrometric (nanoLC-MS/MS), a second extraction was performed with 100% ACN, the supernatants were transferred and reduced completely by evaporation and finally 7 μl of H_2O (0.1% HCOOH) were added.

MALDI-MS Analysis—Mass spectra from 700 to 3500 daltons were carried out on a ULTRAFLEX MALDI TOF/TOF mass spectrometer (Bruker-Daltonik GmbH, Bremen, Germany). The instrument was used at a maximum accelerating potential of 20 kV and was operated in reflector positive mode. Sample preparation was performed with the dried droplet method using a mixture of 0.5 μl of sample and 0.5 μl of matrix solution (α-cyano-4-hydroxycinnamic acid in H_2O/50% ACN diluted 3 times) then the spots were washed with 1 μl of H_2O. Internal calibration was performed with autolysis tryptic peptides, with, respectively, monoisotopic masses at m/z = 842.51, 1045.564, and 2211.105.

NanoLC-MS Analysis—LC-MS/MS analysis of the digested proteins were performed using an CapLC capillary LC system (Micromass) coupled to a hybrid quadrupole orthogonal acceleration TOF MS/MS (Q-TOF II, Micromass Ltd., Manchester, UK). 6 μl of sample was loaded and concentrated onto a C18 PepMap precolumn (LC Packings, Amsterdam, The Netherlands) at a 30-μl/min flow rate and flushed for 3 min with 0.1% ACN before gradient elution of the peptides onto the separating column.

Chromatographic separations were then performed on a 15-cm × 75-μm inner diameter column, packed with C18 PepMap (LC-Packings) stationary phase, with 200 nl/min flow. The elution was performed at 5–45% gradient B (ACN, 0.1% HCOOH, v/v) over 35 min, followed a 95% (solvent B) over 5 min and the re-equilibration of the column was carried out during 20 min by 100% of mobile phase A (H_2O, 0.1% HCOOH, v/v). Mass data acquisitions were piloted by MassLynx software (Micromass) using automatic switching between MS and MS/MS modes as described (30). The electrospray capillary voltage was set to 3.5 kV, the cone voltage set to 40 V, and the source temperature set to 120 °C. The MS survey scan was m/z 300–1500 with a scan time of 1 s and an interscan time of 0.1 s. When the intensity of a peak rose above a threshold of 10 counts, tandem mass spectra were acquired.

Normalized collision energies for peptide fragmentation was set using the charge-state recognition files for +1, +2, and +3 peptide ions. The scan range for MS/MS acquisition was from m/z 50 to 1500 with a scan time of 3 s and a interscan time of 0.1 s. Fragmentation was performed using argon as the collision gas and with a collision energy profile optimized for various mass ranges of ion precursors. The mass data recorded during a nanoLC-MS/MS analysis were processed and converted into MassLynx.pkl format peak lists prior to searching with the search engine Mascot (Matrix Science, London, UK) (31).

MS and MS/MS Data Analysis—The searches were performed with the search engine MASCOT (Matrix Science, London, UK). Searches were done with a tolerance on mass measurements of 30 ppm in MS mode and 0.2 Da in MS/MS mode, 1 missed cleavage, carbamidomethylation, and some variable modifications were taken into account, like methionine oxidation. All proteins present in SWISS-PROT (EXPASY), National Center for Biotechnology Information (NCBI) and TrEMBL (translation of all coding sequences (CDSs) in the EMBL Nucle-

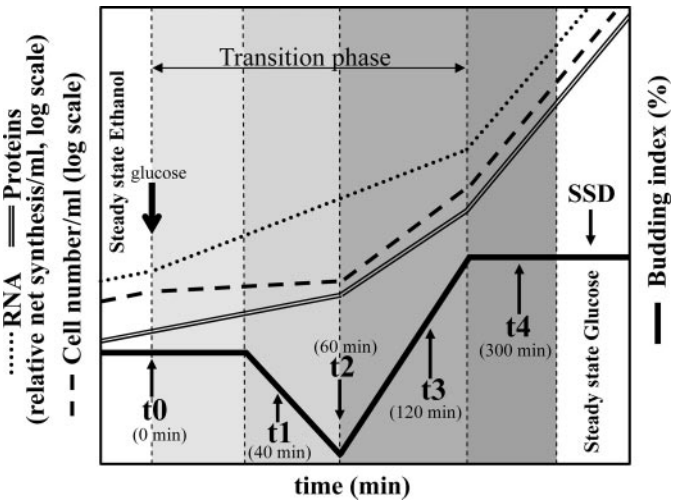

FIGURE 1. **A schematic representation of major events during a nutritional ethanol-glucose shift-up.** The fraction of budded cells, the trend in the rate of RNA and protein synthesis, and increase in cell mass are indicated. Data have been taken from Refs. 22, 23, and 26). In a typical shift-up experiment, 2% glucose is added to cells exponentially growing in medium with 2% ethanol (SCE medium) at time 0. A new steady state is reached several hours after glucose addition. For the proteomics experiments, samples were collected by filtration at different times (as indicated by *arrows*), namely: $t_0 = 0$ min, *i.e.* exponential growth in SCE medium; $t_1 = 40$ min and $t_2 = 60$ min correspond to the midway and the minimum of drop of budding index, respectively; $t_3 = 120$ min correspond to midway increase of fraction of budded cells; $t_4 = 300$ min correspond approximately to the end of transitory state. Finally, a control yeast population exponentially growing on 2% glucose was also collected (SSD).

otide Sequence Data base) data base were used without any pI, M_r, or taxonomy restrictions.

RESULTS

Two-dimensional PAGE of Yeast Proteins during an Ethanol-Glucose Shift-up—To study nutritional shift-up from ethanol to glucose by two-dimensional electrophoresis, 2% glucose was added to wild type cells exponentially growing in Synthetic Complete medium with 2% ethanol (SCE medium). After sugar addition cells were collected by filtration at different times, chosen to sample relevant phases in the time course of the experiment. The chosen time points (summarized in Fig. 1) were: $t_0 = 0$ min, which is exponentially growth in SCE medium, $t_1 = 40$ min and $t_2 = 60$ min correspond to the midway and the minimum of drop of budding index, respectively; $t_3 = 120$ min corresponds to the midway increase of fraction of budded cells; $t_4 = 300$ min corresponds approximately to the end of transitory state. Finally, a control yeast population exponentially growing on 2% glucose was also collected (SSD). Total protein extracts were separated by two-dimensional PAGE and gels were stained with GelCode® (supplemental Fig. S1–S6). The shift-up experiment was performed in triplicate and the six gels of each experiment run simultaneously in the same apparatus. Gel images were compared by PdQuest® 7.1.1 software to evaluate relative and differential protein expression as described under "Experimental Procedures." To discriminate differentially expressed spots we set a 1.5-fold change threshold. Protein spots showing reproducible behaviors in at least two of the three replicate experiments were excised and their identity ascertained by mass spectrometry. In exponential growth in ethanol (t_0 gel) we detected about 600 spots, whereas in exponential growth in glucose (SSD gel) about 500 spots. Among the spots detected in the six gels, 90 spots (plus 48 potentially changed spots) showed different expression levels in at least 1 time point during nutritional shift-up; however, we considered only 76 (plus 35 "potential") spots, in which we identified a single protein, because it was impossible to assess which protein was responsible for spot intensity change in overlapped spots. From these 76 (plus 35 potential) changed spots we identified 63 (plus 29 potential) changed proteins (see supplemental Table S1 for a complete spot list).

Seven of 63 identified proteins were detected within multiple spots: a large part of them appeared as a "train of spot," differing only by their pI, whereas remaining proteins showed a little mass shift (data not shown). This phenomenon indicates post-translational modification or processing which was not further investigated in this work (see supplemental Table S2). Three proteins present as multiple spots showed the same time-dependent pattern of expression: *i.e.* all spots belonging to the same protein were co-regulated. However, in four groups (identifying, Kgd1, Leu4, Adh2, and Ald6) not all spots shared the same pattern of expression. For Kgd1 and Ald6, the differences in observed patterns among some spots are quite small, all of them decreasing although with different kinetics during the transient phase. In the absence of information on molecular differences among the spots, this aspect was not further investigated (for details see supplemental Fig. S7 and Table S2).

Classification of Proteins whose Expression Level Is Modulated during Nutritional Shift-up—Consistently with previous reports using two-dimensional PAGE to study the yeast proteome (13, 32), our analysis identified mostly abundant proteins with large codon bias: no proteins with codon bias values less than 0.1 were detected in this study (data not shown), although the interval with the largest frequency of genes in the entire yeast genome is 0.0 to 0.1 (32). According to YPD, the larger part of proteins identified in this study was localized in the cytoplasm or mitochondrion, 29% of them were either cytoplasmic or nuclear and only 5% were only nuclear (Fig. 2*A*). Therefore, our experimental method, particularly the use of Coomassie staining (GelCode) for protein visualization, allowed us to detect mainly high expressed cytoplasmic proteins, thus limiting our analysis to particular groups of proteins. Not surprisingly, the largest group of proteins that was differentially expressed during nutritional shift-up comprises enzymes involved in intermediary metabolism, notably those in the tricarboxylic acid cycle and carbohydrate, amino acids, and lipid metabolism (Fig. 2*C* and Table S1 and S4). The second largest group of differentially expressed proteins comprised proteins involved in protein synthesis, catabolism, or folding. The cellular roles of other proteins included ones concerning cellular morphogenesis, stress response (notably, oxidative stress response), and other biological functions. Only 2 proteins modulated during the shift-up has no identified function as yet (see later). By *K*-means clustering, we found four major patterns of time-dependent expression among differentially expressed proteins during nutritional shift-up (Fig. 2*B*): linear decrease (pattern I, ↘); linear increase (pattern II, ↗); a tran-

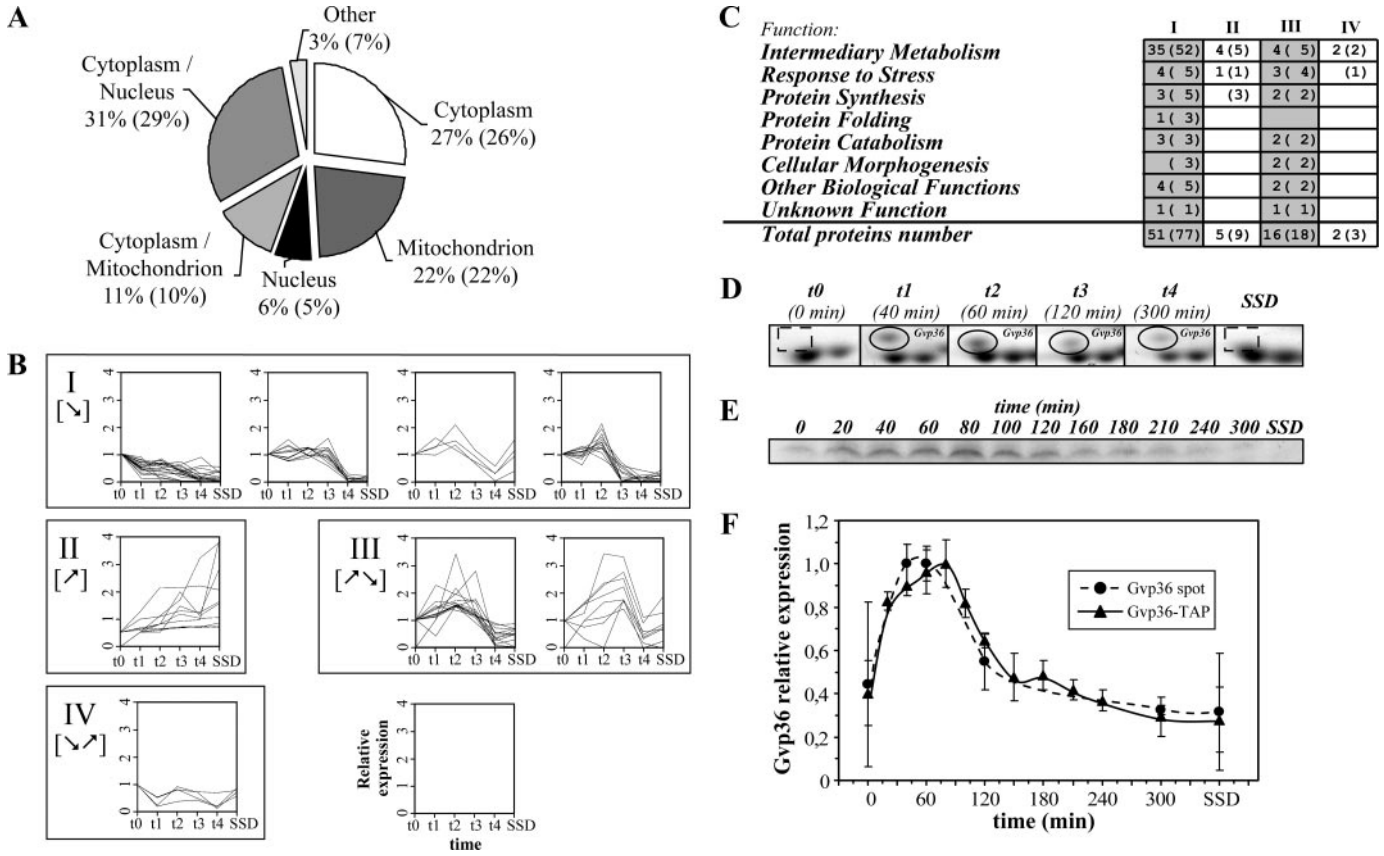

FIGURE 2. **Protein dynamics during the shift-up.** *A*, summary of the subcellular localization of the 63 proteins whose level is modulated during the shift-up. *Number in parentheses* indicate subcellular localization of "changed *plus* potentially changed" proteins. *B*, *K*-means clustering of differentially expressed proteins during a nutritional shift-up. *C*, functional analysis of changed spots in the four behavior classes with different expression profiles during a nutritional shift-up. *Numbers in parentheses* refer to changed *plus* potentially changed spots. *D*, pattern of expression of Gvp36. Gel images of the Gvp36 spot during a nutritional shift-up from ethanol to glucose in wild type cells. In the experiment shown, Gvp36 was undetectable in both EtOH medium (t_0) and glucose media (SSD), it appeared after glucose addition (t_1) and increased its intensity in the middle of the adaptation period (t_2), although was not detected in the new steady state (SSG). *E*, Gvp36-TAP tagged expression during a nutritional shift-up. Glucose was added to Gvp36-TAP cells growing on ethanol and cellular samples were collected at the indicated time points. Western blot analysis was performed using anti-TAP antibodies. *F*, quantification of Gvp36 expression. Densitometric analysis was performed on the Gvp36 spots from bidimensional gels and on bands corresponding to Gvp36-TAP-tagged proteins. Values are relative to the maximum level of expression measured. Data reported are average ± S.D. of three (Gvp36 spots) or two (Gvp36-TAP) independent experiments.

sient peak of expression (pattern III, ↗↘); a transient decrease of expression (pattern IV, ↘↗).

Most enzymes involved in the tricarboxylic acid cycle, including aconitase, citrate synthase, isocitrate dehydrogenase, succinate dehydrogenase, succinate CoA ligase, and α-ketoglutarate dehydrogenase followed pattern I (↘), *i.e.* they decreased more or less linearly during the time course of the experiment, in keeping with the shift from respiratory to fermentative metabolism. The same pattern was displayed by the rate-limiting gluconeogenic enzyme fructose 1,6-bisphosphatase. Consistently with the respective physiological role, alcohol dehydrogenase II, involved in ethanol utilization was linearly down-regulated (pattern I, ↘), whereas alcohol dehydrogenase I, involved in acetaldehyde reduction, was linearly up-regulated (pattern II, ↗). Enolase II increased linearly (pattern II, ↗), whereas Tdh3 (encoding glyceraldehyde-3-phosphate dehydrogenase) was transiently up-regulated (pattern III, ↗↘), and Tif1, involved in translational initiation, showed a pattern III (↗↘) in keeping with the need for increased translation in glucose-containing media.

Quite a large number of modulated proteins were involved in response to stress, particularly oxidative stress. *CCP1*-encoded cytochrome *c* peroxidase 1 and Tsa1, a protein that protects cells from free radical damage and acts as a molecular chaperone following oxidative stress, showed a transient peak of expression (pattern III, ↗↘). Rhr2, an isoform of glycerol phosphatase required for glycerol biosynthesis and involved in the cellular response to osmotic, anaerobic, and oxidative stress was the only stress-related protein that increased linearly during the shift-up (pattern II, ↗). All other stress-related proteins, including Hsp78, Nce103, and Pil1, linearly decreased during the shift. These results are summarized in Fig. 2*C* and Table S1.

Identification of Gvp36 as a Protein That Is Transiently Up-modulated during the Shift-up—Among spots that were called changed (or potentially changed, see "Experimental Procedures") during the nutritional shift-up, we focused on those with a peak or a minimum of intensity corresponding to the minimum in the fraction of budded cells (trends III (↗↘) and IV (↘↗), respectively). This behavior suggested that the proteins detected in these spots are involved in metabolism regulation during the change of carbon source. Among them (Adh2, Ald6, Atp2, Ccp1, Cpr1, Dps1, Gdh3, Gvp36, Hsp82, Kgd1, Leu4, Lia1, Met6, Mls1, Pre9, Rnr4, Sgt2,

Tdh3, Tif1, Tsa1) only one protein had an unknown function: Gvp36.

In two of three experiments the spot detected as Gvp36, whose identity was confirmed by MS/MS analysis (data not shown), had the same intensity in exponential growth in glucose as in exponential growth in ethanol, whereas in the third replicate the protein was undetectable in samples prepared during exponential growth in both media. A blow-up of a gel from the latter experiment is reported in Fig. 2*D*, because it allows a better visual appreciation of the pattern of Gvp36 accumulation, *i.e.* increased accumulation in the midway of adaptation. To further validate this result, we examined the pattern of Gvp36 accumulation during a nutritional shift-up in a *GVP36-TAP*-tagged strain. Levels of the tagged proteins were evaluated by Western blot analysis using anti-TAP antibodies (Fig. 2*E*). Fig. 2*F* reports the densitometric analysis (average ± S.D.) performed on the bands corresponding to Gvp36-TAP and on the Gvp36 spots from bidimensional gels: both measurements confirm a clear transient accumulation of Gvp36 during the adapative phase of the nutritional shift-up.

Gvp36 is an unknown function protein coded by the *YIL041w* gene and termed as "Golgi vesicle protein of 36 kDa" because of its immunoisolation in Golgi subcompartments (33). Gvp36 gives an immunofluorescent staining compatible with Golgi localization (34). In *S. cerevisiae*, Gvp36 shares 24% sequence identity with Ypr148c, a protein of unknown function. Null mutants in the Ypr148c-encoding gene show incorrect meiotic cell cycle progression (35). Proteins homologous to Gvp36 are found in *Schizosaccharomyces pombe*, *Candida albicans*, and other yeasts, but no information on their functional properties is available so far. No Gvp36-homologous proteins are found in higher eukaryotes.

Bioinformatic Analysis Identifies a BAR Domain in Gvp36—Different bioinformatic tools predicted that Gvp36 contains a BAR domain: NCBI RPS-BLAST predicted a BAR domain between residues 163 and 292; ORFEUS (provided by Yeast Research Center, YRC) confidently predicted an Arfaptin domain between residues 114 and 326; SMART tool predicted a BAR domain between residues 10 and 299, albeit with a border line *E*-value. Finally, 3D-JIGSAW, an automated system to build three-dimensional models for proteins based on homologues of known structure, assigned the entire Gvp36 protein to the human Endophilin 1 BAR domain three-dimensional structure.

The BAR (Bin1, Amphiphysin, and Rvs167) domain is the most conserved feature in amphiphysins from yeast to human and is also found in endophilin and arfaptins (36). However, sequence homology between known BAR domains is relatively modest (37). BAR domain proteins have been implicated in an extraordinary diversity of cellular processes that generate membrane curvature, including cell polarity, endocytosis, regulation of the actin cytoskeleton, and secretory vesicle fusion. Structural analysis of BAR domain revealed that it is a banana-shaped dimer formed by monomers (36), able to bind and/or bend membranes (38). Consistently with its assignment to the class of BAR-containing proteins, Gvp36 dimerizes with itself on the basis of two-hybrid tests (39) as BAR-containing proteins (37, 40).

Yeast has two known BAR domain proteins, Rvs167 and Rvs161 (according to SMART data base) (37, 40). Mutants in the RSV gene were isolated because they exhibit reduced viability upon starvation. The two proteins have strong amino acid sequence homology and their mutation causes a phenotype consistent with a role for the Rvs proteins in vesicle trafficking, cortical actin cytoskeleton, and endocytosis. Experiments described below were thus designed to compare phenotypes of *gvp36*Δ mutants with those of mutants in the genes encoding known yeast BAR-containing proteins, *i.e. RSV161* and *RSV167*.

*gvp36*Δ *Is Defective in Adaptation to Changes in Nutrient Concentration*—During the transitory phase of an ethanol to glucose shift-up, Gvp36 expression peaks in correspondence with the minimum of budding index. If Gvp36 plays an active role during the shift-up, then a defect of a *gvp36*Δ strain during the adaptation phase should show up as a failure to down-regulate budding during the initial phase of a shift-up, which we identified as a landmark event. Preliminary experiments showed that formation of *gvp36*Δ colonies on YP and SC solid media supplemented with 3% glycerol was delayed compared with wild type cells and that little or no growth of the *gvp36*Δ mutant was detectable in ethanol containing media (data not shown). Because *gvp36*Δ mutant does not grow in media supplemented with ethanol as a sole carbon source, we followed a glycerol to glucose shift-up. In wild type strain a drop of budding index took place an hour after glucose addition (Fig. 3*A*, *triangles*), whereas no drop in budding index was apparent in *gvp36*Δ cells (Fig. 3*A*, *squares*), indicating that lack of Gvp36 induces a defect in the adaptation to a new carbon source.

The above observation prompted us to examine whether *gvp36*Δ cells could cope successfully with withdrawal of either the nitrogen or the carbon source. Nitrogen deprivation arrests cells in $G_{0/1}$ phase (41, 42). Cells grown in YPG were collected by filtration, washed, and resuspended in minimal medium supplemented with yeast nitrogen base without ammonium sulfate and 3% glycerol. Fig. 3*B* shows that within 24 h, wild type stopped growth as unbudded cells, whereas the arrested *gvp36*Δ strain had about 20% of budded cells, suggesting a defect also in nitrogen starvation adaptation. *gvp36*Δ cells also showed a delay in recovery from nitrogen starvation (Fig. S8, *A* and *B*).

We then tested the ability of *gvp36*Δ cells to grow with decreasing glucose concentrations. Wild type and mutant cells, exponentially growing in YPD, were serially diluted and spotted onto YNB solid medium containing 2, 0.5, 0.25, 0.1, or 0.05% glucose. Wild type grew well in all conditions, whereas *gvp36*Δ mutant grew slower and slower with reduction of available glucose, virtually stopping growth after 2 days in YNB solid medium supplemented with 0.05% glucose (Fig. 3*C*).

Finally, we followed entry into stationary phase after glucose exhaustion. Wild type and *gvp36*Δ cells were grown to saturation in YPD medium and samples were removed daily for analysis of cell growth (Fig. 3*D*), budding index (Fig. 3*E*), and cell viability (Fig. 3*F*), assayed as ability to form colonies on YPD medium. At the concentration of about 1×10^8 cells/ml wild type cells ceased rapid growth and underwent a very slow dou-

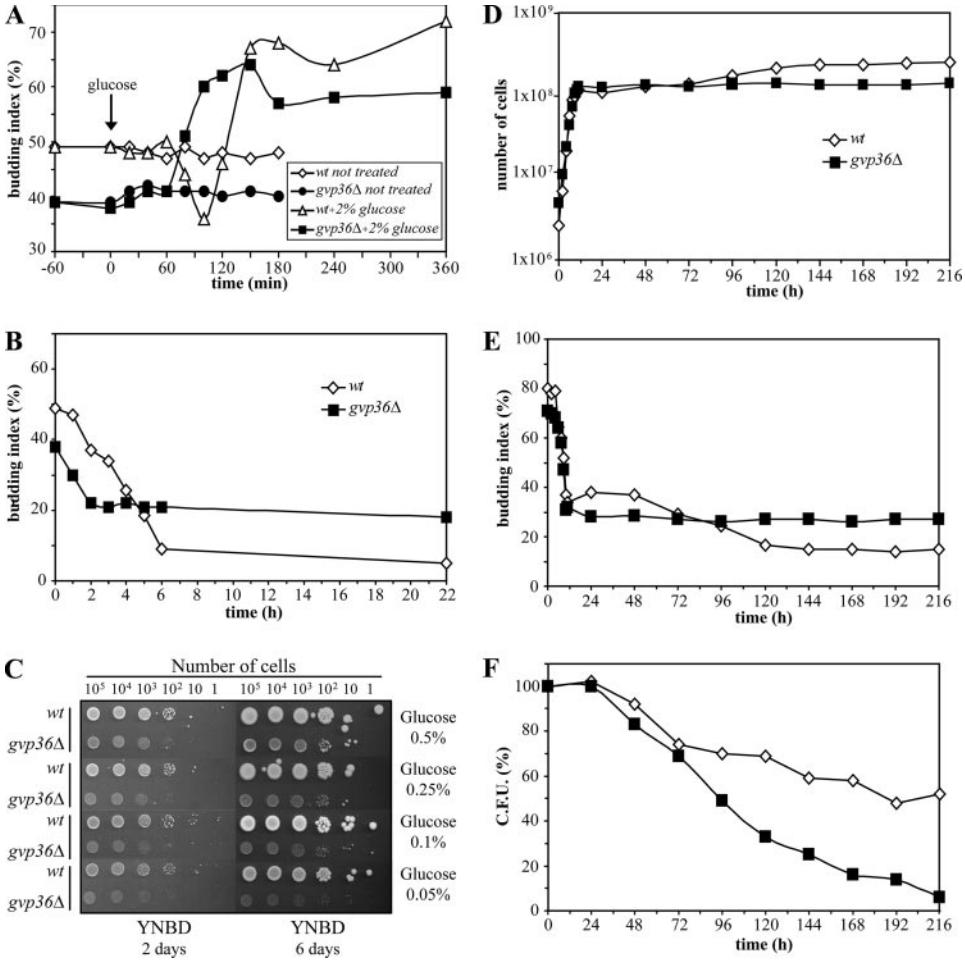

FIGURE 3. ***gvp36Δ* mutant shows a defect in adaptation to changes in nutrient concentration.** *A*, 2% glucose was added to cells growing in YP, 3% glycerol and samples were collected to evaluate the percentage of budded cells in wild type (*triangles*), *gvp36Δ* (*squares*), non-treated wild type (*diamonds*), not treated *gvp36Δ* (*circles*). *B*, cells grown in YPG were collected by filtration, washed, and resuspended in minimal medium supplemented with yeast nitrogen base without ammonium sulfate and 3% glycerol: samples were collected to evaluate budding index. *C*, wild type and *gvp36Δ* cells, exponentially growing in YPD, were serially diluted and spotted onto YNB solid medium supplemented with different glucose concentrations (0.5, 0.25, 0.1, and 0.05%) and incubated at 30 °C. *D–F*, wild type and *gvp36Δ* mutant were grown to saturation in YPD medium and samples were removed daily for analysis of cell growth (*D*), budding index (*E*), and cell viability (*F*).

bling over a period of 6 days before finally ceasing proliferation, with 15% of budded cells. As cells entered a state of deeper and deeper chronological aging, viability decreased, reaching a value of 50% on day 9 of the experiment. On the contrary, *gvp36Δ* cells already ceased growth after the first day and their viability decreased substantially as they entered deeper and deeper stationary phase, reaching a value of about 5% on day 9 of the experiment. These data correlate well with reduced heat shock resistance of growth-arrested *gvp36Δ* (Fig. 6*B*).

The gvp36Δ Mutant Is Unable to Grow in Ethanol and Presents a Slow Growth Phenotype in Glucose- and Glycerol-supplemented Media—To established if this mutant was unable to use ethanol as carbon source or if it had a higher sensitivity to ethanol, wild type and mutant cells, exponentially grown in YPD, were serially diluted and spotted onto YP solid medium containing glucose alone or glucose plus either 2 or 4% ethanol. Because in these conditions glucose is used as a preferential carbon source, no effect on growth of wild type is apparent, as expected. On the contrary, ethanol slowed down growth of the *gvp36Δ* mutant at both tested concentrations (Fig. 4*A*).

The effect of ethanol (2% final concentration) on cells growing in glucose-supplemented YP liquid medium was then tested. Ethanol had no major effects on growth and budding of wild type cells (Fig. 4*B*, *diamonds* and *triangles*, respectively). On the contrary, a significant drop in cell growth and budding of the *gvp36Δ* mutant was observed (Fig. 4*B*, *circles* and *squares*, respectively). Because viability of ethanol-treated *gvp36Δ* cells, tested by counting colony forming units of samples taken at different times after addition of ethanol, showed only a transient minor decrease within the first 4 h of treatment (Fig. 4*C*), ethanol appears to be cytostatic rather than cytotoxic for the *gvp36Δ* mutant.

Wild type and *gvp36Δ* were grown in liquid YP medium supplemented with either 2% glucose (YPD) or 3% glycerol (YPG). Duplication time (T) and budding index (BI) were scored by electronic counting and direct microscopic examination, respectively (Fig. 5*A*). The fraction of S + G_2 + M cells and distribution of protein content in the population were analyzed by flow cytometry (Fig. 5, *A* and *B*). Mutant cells had a longer duplication time in both media that was accompanied by a moderate, but significant decrease in BI and in the fraction of S + G_2 + M cells. YPD-, but not YPG-grown, *gvp36Δ* cells were smaller than wild type. These data could indicate that the absence of Gvp36 alters nutritional modulation of cell growth/cell cycle coordination. Notably, the decrease in BI and in the fraction of S + G_2 + M cells could result from a delayed G_1 to S transition and/or delayed exit from mitosis, as suggested by experiments using cells synchronized by α-factor and nocodazole treatment or nitrogen starvation (see supplementary materials Fig. S8, *C* and *D*).

gvp36Δ Mutant Has Normal Osmotic Shock Response and Reduced Heat Shock Resistance—Although ethanol is a final product of anaerobic fermentation of sugar by yeast, it is somehow toxic to yeast cells and induced stress responses such as the expression of heat shock proteins (43). Because the higher sensitivity of the *gvp36Δ* mutant to ethanol could be caused by a defect in stress response, mutant sensitivity to osmotic and heat stresses was investigated.

To test osmotic stress resistance, wild type and mutant cells, exponentially growing in YPD, were serially diluted and spotted

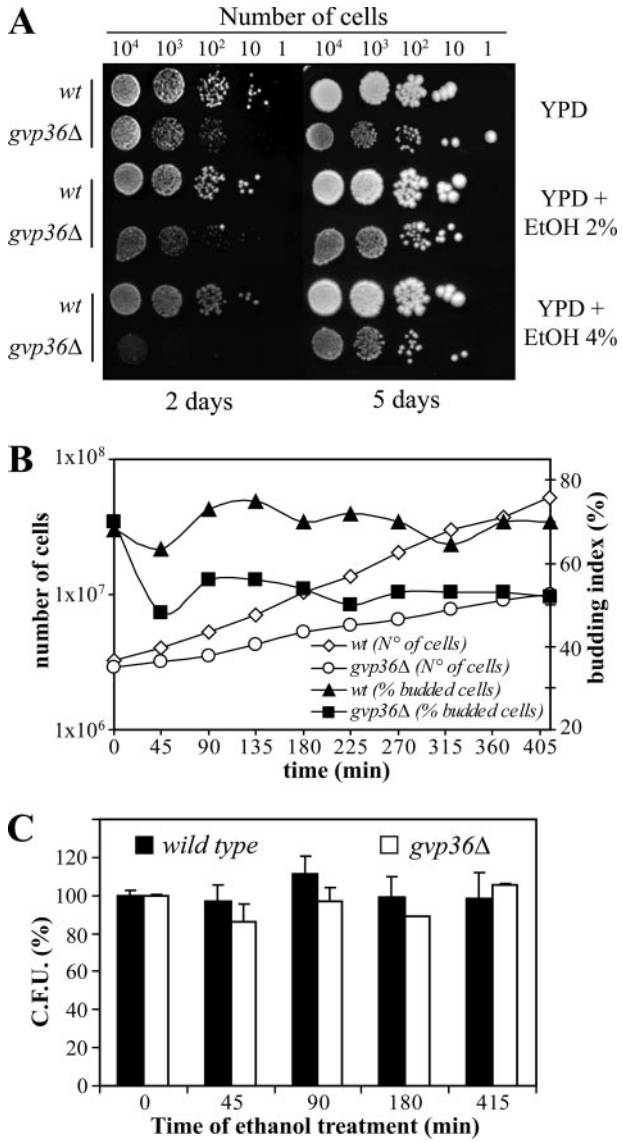

FIGURE 4. ***gvp36Δ* mutant shows altered sensitivity to ethanol.** *A*, wild type and *gvp36Δ* cells, exponentially growing in YPD, were serially diluted and spotted onto YP solid medium containing glucose as preferential carbon source and either 2 or 4% ethanol, and plate images were acquired after 2 and 5 days of growth. *B*, 2% ethanol was added to wild type and *gvp36Δ* cells exponentially growing in YP medium with 2% glucose and samples were collected to evaluate the percentage of budded cells (wild type, *triangles*; *gvp36Δ*, *squares*) and growth rate (wild type, *diamonds*; *gvp36Δ*, *circles*). *C*, wild type (*black*) and *gvp36Δ* (white) cell viability after ethanol added was assessed by counting colony forming units: percentages are relative to time 0 of the experiment.

A

medium	Parameters	Strain	
		wt	*gvp36Δ*
YPD	T (min)	84 ± 3.1 (n = 3)	120 ± 13.1** (n = 3)
	BI	77 ± 3.7 (n = 17)	70 ± 2.9** (n = 17)
	% S+G2+M	83 ± 1.5 (n = 5)	75 ± 1.9** (n = 5)
	P (Ch #)	520 ± 15.9 (n = 3)	424 ± 5.9** (n = 3)
YPG	T (min)	285 ± 13.6 (n = 3)	425 ± 13.0** (n = 3)
	BI	50 ± 1.1 (n = 24)	44 ± 5.6** (n = 24)
	% S+G2+M	62 ± 0.6 (n = 3)	43 ± 1.2** (n = 3)
	P (Ch #)	438 ± 13.6 (n = 4)	395 ± 18.9 (n = 4)

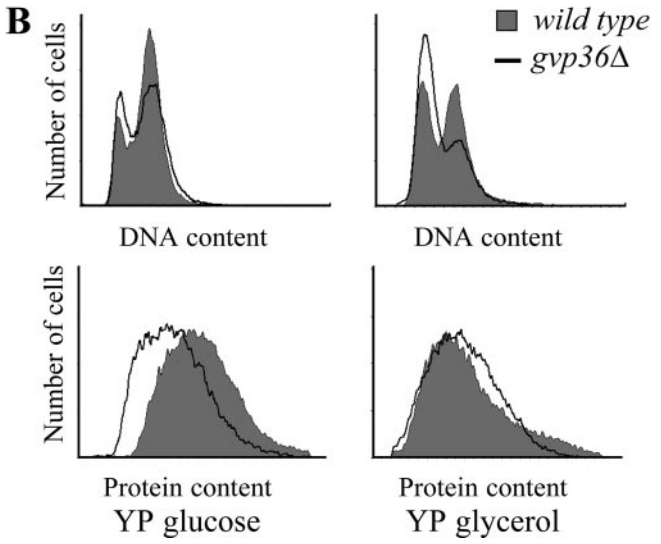

FIGURE 5. ***gvp36Δ* mutant shows a growth defect.** *A*, duplication time (*T min*), budding index (*BI*), percentage of S + G_2 + M cells, and average protein content determined by flow cytometry (*P*) were determined for wild type cells and for *gvp36Δ* mutant exponentially growing in YP medium either with 2% glucose (YPD) or with 3% glycerol (YPG). All results are expressed as mean ± S.D. **, indicates that the difference between wild type and *gvp36Δ* mutant is statistically highly significant (Student's *t* test; $p = 0.01$). *B*, DNA and protein content distribution determined by flow cytometry for wild type cells and for *gvp36Δ* mutant cells exponentially growing in YP medium either with 2% glucose (YPD) or with 3% glycerol (YPG).

onto YPD solid medium supplemented with different sorbitol concentrations. Results reported in Fig. 6*A* indicate that *gvp36Δ* cells grow somehow slower than wild type regardless of the presence of increasing concentrations of sorbitol.

To test heat shock resistance, cells grown for either 2 or 7 days in YPD medium were treated at 51 °C for 5, 10, 15, or 20 min and then colony forming units formed on YPD plates scored. The *gvp36Δ* mutant was more heat shock sensitive than wild type, the more so when cells were scored at the later time points (Fig. 6*B*).

gvp36Δ Mutant Is Thermosensitive for Growth at 37 °C—Cells, exponentially growing in YPD, were serially diluted and spotted on YPD and YNBD solid medium; at the same time cells were plated on the same media, shifted at 37 °C, and colony forming units formed were scored. On YPD *gvp36Δ* mutant had an important reduction of growth rate and viability, whereas on YNBD virtually no growth was observed; notably 1 M sorbitol added to the medium rescued the mutant (Fig. 6*C*). Mutant growth was also affected during the shift from 30 to 37 °C in YNBD liquid medium: indeed after temperature perturbation the wild type strain continued to grow and reached stationary phase, whereas the *gvp36Δ* mutant stopped dividing after one

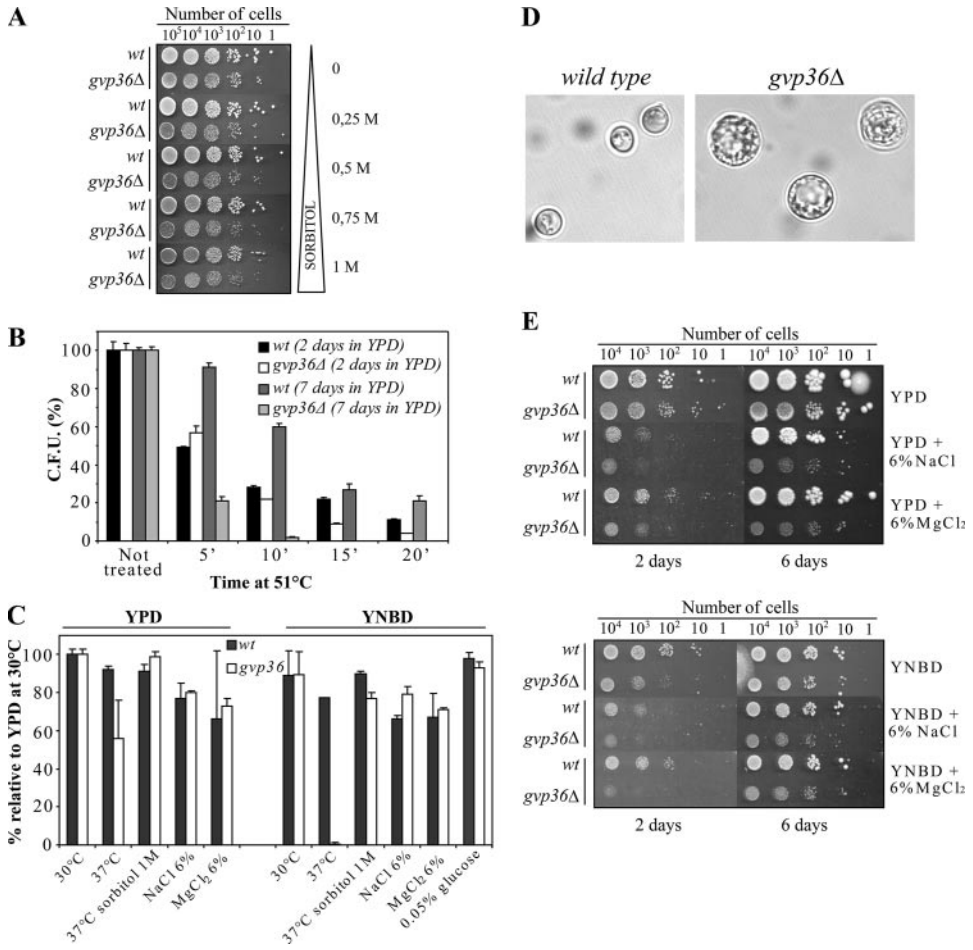

FIGURE 6. **Stress resistance of *gvp36*Δ cells.** *A*, wild type and *gvp36*Δ cells, exponentially growing in YPD, were serially diluted and spotted onto YPD solid medium supplemented with different sorbitol concentrations. *B*, confluence grown cells (about 1–2 × 10^8 cells/ml, grown 2 days in YPD medium) were treated at 51 °C for 5, 10, 15, or 20 min and then plated onto YPD solid medium: their viability was assessed by colony forming units (*CFU*) (percentages are relative to the control). *C*, wild type and *gvp36*Δ cells, exponentially growing in YPD, were plated onto YPD or YNBD solid medium, supplemented or not supplemented with sorbitol, and shifted to 37 °C; otherwise, wild type and *gvp36*Δ cells, exponentially growing in YPD, were plated onto YPD or YNBD solid medium supplemented with 6% NaCl or $MgCl_2$ and incubated at 30 °C: viability was assessed by counting colony forming units (*CFU*) (percentages are relative to wild type in YPD medium at 30 °C). *D*, wild type and *gvp36*Δ cells, exponentially growing in YNBD, were shifted from 30 to 37 °C; after 20 h cells were collected and cell images were acquired. *E*, wild type and *gvp36*Δ cells, exponentially growing in YPD, were serially diluted and spotted onto YPD or YNBD solid medium supplemented with 6% NaCl or $MgCl_2$ and incubated at 30 °C.

or two division cycles; after 20 h the *gvp36*Δ mutant had abnormally large cells with a lot of granules, with the same percentage of budded cells than wild type (Fig. 6*D*). Therefore, *gvp36*Δ mutant is also thermosensitive for growth at 37 °C, a phenotype often found in mutants in endocytosis/cell wall biogenesis/vesicle trafficking (37, 44).

*gvp36*Δ *Mutant Is Sensitive to High Salt Concentration*—Because yeast mutants in the endocytosis pathway are often unable to grow on medium with high salt concentrations (45), we tested the ability of *gvp36*Δ to grow on medium with high salt concentration. Wild type and mutant cells, exponentially growing in YPD, were serially diluted and spotted onto YPD and YNBD solid medium supplemented with 6% NaCl or 6% $MgCl_2$; furthermore, cells were plated on the same media and counting forming units formed were scored. On both media, with both salts, *gvp36*Δ mutant showed a major growth defect (Fig. 6*E*), but no alteration in viability compared with wild type (Fig. 6*C*).

*gvp36*Δ *Mutant Is Defective in Polarization of the Actin Cytoskeleton*—Actin cytoskeleton has a role in protein secretion (46) and several endocytosis mutants have defects in its organization. Yeast actin cytoskeleton is organized in cortical patches and cytoplasmic cables (45) and its distribution is cell cycle-specific: during bud emergence and bud growth, actin patches concentrate in the bud, whereas during cytokinesis, actin patches are equally distributed between mother and daughter cell (47). To visualize actin cytoskeleton distribution, we stained actin with rhodamine-conjugated phalloidine in exponentially growing cells in YPD (Fig. 7*A*). As expected, most of wild type cells (92%) showed actin patches concentrated at the growing bud; in contrast, the *gvp36*Δ mutant showed 34% of cells with 50–90% of actin patches in the bud (partially depolarized cells) and 15% of cells with less than 50% of their actin patches in the bud (totally depolarized cells), showing a defect in the polarization of its cytoskeleton (Fig. 7*B*).

Latrunculin-B binds to monomeric G actin and inhibits actin polymerization; because hypersensitivity to latrunculin has been reported for mutants in genes encoding actin-binding protein and is indicative of an unstable actin network, we tested sensitivity of wild type and *gvp36*Δ mutant to this drug, using a halo assay with different Lat-B concentrations (0, 1, 2, and 4 mM). Surprisingly, *gvp36*Δ mutant was more resistant than wild type to Lat-B (Fig. 7*C*); this phenotype could indicate that Gvp36 is involved in actin dynamics and in destabilization of the actin cytoskeleton: indeed, Latrunculin sequesters actin monomers without increasing the off rate of actin from filaments, and a mutant that can increase actin filament turnover could confer Latrunculin resistance (48, 49).

*gvp36*Δ *Shows Severe Defects in Vacuole Biogenesis and in Fluid Phase Endocytosis*—To investigate whether *GVP36* deletion affects endocytosis, we use two different dyes, LY and FM4-64, to stain vacuoles of cells exponentially growing in SCD medium. To assess fluid phase endocytosis we followed the uptake of LY (Fig. 8*A*): in wild type cells this dye accumulated in the vacuoles after its internalization; in *gvp36*Δ mutant cells, instead, we observed a dramatic decrease in Lucifer yellow uptake. Mutant images taken with the same acquisition time as the images of wild type cells did not show any detectable stain-

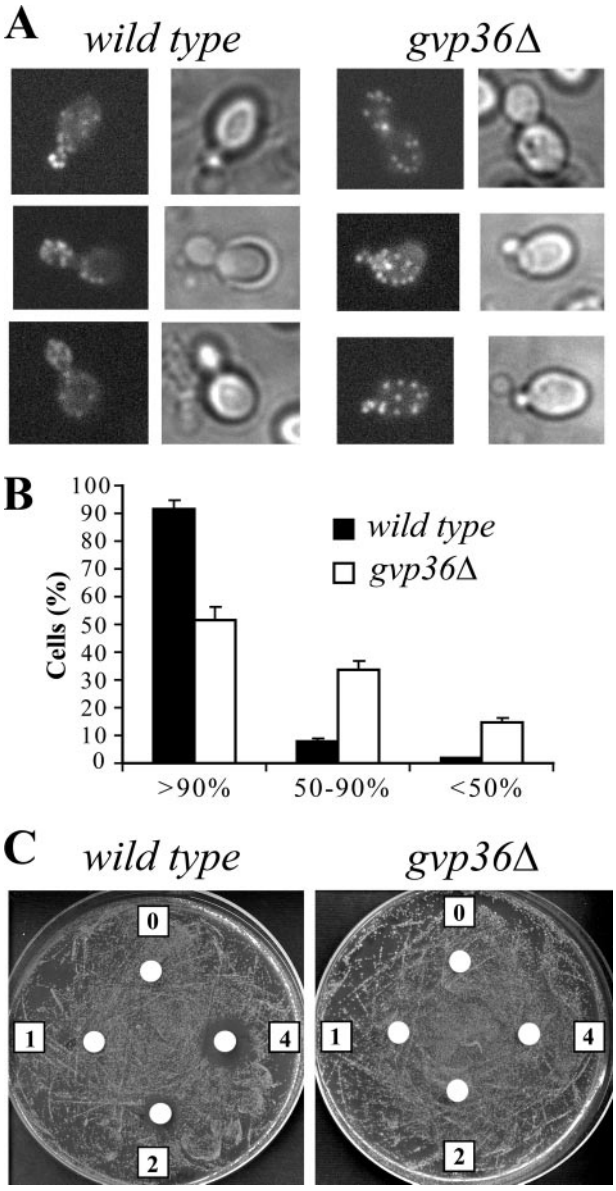

FIGURE 7. ***gvp36*Δ mutant is defective in polarization of the actin cytoskeleton.** *A* and *B*, cells, exponentially growing in YPD, were fixed and their actin stained using rhodamine-conjugated phalloidin. *A*, representative cells from each strain are shown. *B*, percentage of cells with depolarized actin is shown (wild type, *black columns*; *gvp36*Δ mutant, *white columns*) ~100 small- and medium-budded cells were scored as having: >90% of their actin in the bud; 50–90% of their actin in the bud; or <50% of their actin in the bud. *C*, Lat-B was placed on a sterile disk at concentrations of 0, 1, 2, and 4 mM. These disks were placed on nascent lawns of wild type and *gvp36*Δ mutant, then allowed to grow at 30 °C for 2 days.

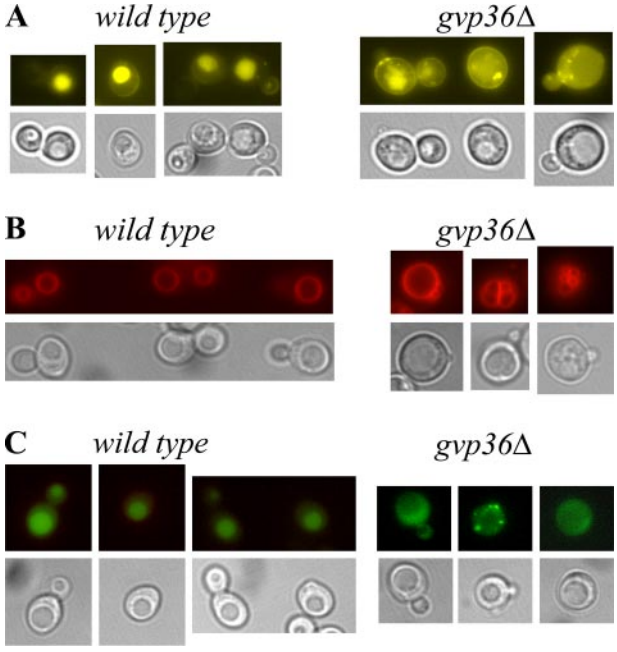

FIGURE 8. ***gvp36*Δ mutant has severe defects in fluid phase endocytosis and in vacuole biogenesis.** The three different vacuole stainings were performed as described under "Experimental Procedures" on wild type and *gvp36*Δ mutant, exponentially growing in SCD. Shown are the same field of cells viewed with Nomarski and fluorescence optics. *A*, Lucifer yellow uptake. *B*, FM4-64 uptake. *C*, CDCFDA vacuole staining.

ing; however, by overexposing the images, we could identify either several small vacuoles or some small patches near the cell wall. To determine whether there were defects in membrane trafficking as well as in the initial steps of endocytosis, we followed the uptake of the lipophylic dye FM4-64 (Fig. 8*B*). Whereas virtually all wild type cells showed a large single vacuole in mother cell and a large vacuole in daughter cell, about two-thirds of *gvp36*Δ cells showed more than three small vacuoles, whereas the remaining one-third showed a large vacuole flanked by several very small vacuoles.

Vacuole biogenesis defect in the *gvp36*Δ mutant was confirmed by staining the vacuole lumen with CDCFDA (Fig. 8*C*), a dye that enters vacuoles independently of the endocytic pathway and is required to be processed in the vacuole to stain this organelle: in fact, this dye is membrane permeable until nonspecific esterases hydrolyze the acetate groups to form more highly charged, less membrane-permeable compounds (50). As with FM4-64, all wild type cells showed a large single vacuole in mother cell and a large vacuole in daughter cell; on the contrary, *gvp36*Δ mutant cells did not show any vacuolar staining, but a diffuse staining with occasional patches near the cell wall, suggesting that vacuoles were not well formed and did not contain the processing enzyme.

Therefore, *gvp36*Δ mutant showed severe defects in vacuole biogenesis and in fluid phase endocytosis, but, at least after a long dye incubation time, showed normal vacuole labeling by FM4-64: this phenotype, LY negative, FM4-64 positive staining, was also observed in two secretion defective yeast mutants, *sec18* (blocked in endoplasmic reticulum to Golgi transport at restrictive temperature) and *sec14* (Golgi blocked at restrictive temperature), and in two endocytosis mutants *end3* and *end4* (51) (notably, *end3-1* mutant is Latrunculin resistant (49)).

DISCUSSION

About 10 years after the yeast genome was fully sequenced (52), and despite the large efforts of the scientific community and the development of more and more sophisticated genome-wide techniques, the function of a large number of yeast genes remains elusive and knowledge of most genes of "known" function is exceedingly poor and contrasts with the deep knowledge of the relatively few, very well characterized genes (53). Efforts coupling genome-wide techniques to specifically tailored experiments may help to link genes of unknown function to

specific cellular processes. In the experiments reported in this paper, a proteomic analysis of a nutritional ethanol-glucose shift-up was undertaken. Unlike the diauxic shift, in which progressive and reciprocal changes in glucose and ethanol take place, during a nutritional shift-up the change in carbon source takes place abruptly and cells employ several hours to adapt to the novel, richer carbon source (22, 23, 26). We used the change in budding index as a guide to choose appropriate, relevant time points during the transitory phase for preparation of samples for the analysis of proteome by two-dimensional electrophoresis followed by mass spectrometry.

The novelty of our paper regards both a more accurate description of the dynamics of protein expression during a shift-up and the identification of Gvp36, a protein of previously unknown function, as a BAR-containing protein substantially modulated during the shift-up and involved in vesicular traffic.

Dynamics of Protein Expression during the Shift-up—Among the ~600 spots detected in the six gels, 90 spots (plus 48 potentially changed spots) showed time-dependent changes in expression during the shift-up; in 76 spots (plus 35 potentially changed spots) we identified a single protein. Our experimental method allowed us to detect mainly high expressed cytoplasmic and mitochondrial proteins: not surprisingly, the largest group of proteins that was found to be differentially expressed during nutritional shift-up comprises enzymes involved in tricarboxylic acid cycle and in carbohydrate, amino acids, and lipid metabolism. Of great interest is the finding that the shift-up transition induces the modulation of a substantial number of proteins involved in the response to stress, mainly oxidative stress. Various dynamics of response are observed: a transient peak of expression for cytochrome *c* peroxidase 1 and Tsa1, a protein that protects cells from free radical damage, a linear decrease for superoxide dismutase and for chaperone Hsp78, whereas the glycerol phosphatase Rhr2, which is involved in glycerol biosynthesis and in the cellular response to various kinds of stress increased linearly during the shift-up (1, 21, 54).

The sensitivity of our proteomic analysis does not allow us to study proteins present in low amounts, such as those driving the cell cycle that is clearly modulated during the shift-up (23). An increase of cyclin Cln3 expression that peaks when the budding index drops has been reported by Alberghina *et al.* (26). Also, Far1, the cyclin-dependent kinase inhibitor reported to interplay with Cln3 in the G_1 to S network in the cited paper increases during shift-up so that the Cln3/Far1 ratio reaches a maximum when the budding index is at its minimum. Taken together these data are consistent with the notion that cells at the onset of shift-up delay entrance into S phase and recover when the budding index increases. This fact partially synchronizes the budding cycle of cells of the population as compared with steady states.

Identification of Gvp36 as a BAR-containing Protein Involved in Vesicular Traffic and in Nutritional Adaptation—We propose that Gvp36, whose synthesis is transiently up-regulated during shift-up, represents a novel yeast BAR protein, because not only different bioinformatic tools predict that Gvp36 has a BAR domain (see "Results"), but *gvp36*Δ mutants share several phenotypes with mutants in *RSV161* and *RSV167*, *i.e.* the genes encoding the two previously known yeast BAR proteins (refer to the recent review by Ren *et al.* (37), and references cited therein for phenotypes of *rsv* mutants). These phenotypes include: (i) general growth defects, notably on non-fermentable C source: *gvp36*Δ grows poorly on glycerol (Fig. 5), whereas ethanol is cytostatic (Fig. 4); (ii) heat shock sensitivity and poor growth at 37 °C. The latter phenotype of *gvp36*Δ is corrected by adding 1 M sorbitol to the growth medium, as is typical of mutants defective in cell wall biogenesis, endocytosis, and vesicular traffic (37, 44); (iii) sensitivity to high salt concentration (45): *gvp36*Δ cells grow slowly in the presence of 6% NaCl and 6% $MgCl_2$ (Fig. 6*E*) but remain viable (Fig. 6*C*). High salts induce fast transient actin depolymerization (55). *gvp36*Δ may be slow in recovery (see (iv) below); (iv) defect in polarization of the actin cytoskeleton and altered sensitivity to latrunculin. *gvp36*Δ cells show partially delocalized actin cytoskeleton and resistance to latrunculin (Fig. 7), suggesting that Gvp36 may affect actin polymerization/depolymerization dynamics, possibly by increasing actin turnover of actin filaments (48, 49). (v) Defects in endocytosis and vacuolar biogenesis. The yeast vacuole is known to receive material from biosynthetic vesicular traffic from the Golgi apparatus and endocytic vesicular traffic from the cell surface, the two pathways merging before vacuolar delivery (44). Results reported in Fig. 8 that make use of FM4-64, CDCFDA, and LY indicate that *gvp36*Δ cells have the same FM4-64 positive, LY-staining pattern shown by *sec18* (blocked in endoplasmic reticulum-Golgi transport), *sec14* (blocked in Golgi transport), *end3* and *end4* (defective in α-factor internalization) (51). *Sec1* (blocked in the fusion between vesicles and plasma membrane) is negative to staining with both dyes. Lack of staining with CDCFDA could result from a defect in localization of the dye-processing enzyme, whereas vacuolar fragmentation could be due to a defect in vesicle fusion/distribution (51, 56). (vi) Defects in entering stationary phase upon glucose or nitrogen starvation (Fig. 3, *A* and *B*). It is known that the actin-endocytosis complex is required for cells to cease cell division in response to nutrient stress, possibly because endocytosis could result in the internalization of membrane proteins required for growth and budding and/or because fluid-phase endocytosis could be required for the uptake of growth inhibitory small molecules from the medium (57). All these phenotypes are compatible with known BAR domain functions in binding and/or bending cellular membranes (37).

Regulation of Gvp36 Expression—The spot detected as Gvp36 was at or below the limit of detection in both ethanol and glucose media and reproducibly showed a peak of expression in correspondence to the minimum of budding index. A previous study about mRNA and protein abundance in *S. cerevisiae* exponentially growing in ethanol and galactose-supplemented media did not show any significant change in the expression of Gvp36 encoding mRNA in the two conditions (14). Moreover our investigation on *GVP36* mRNA levels by GeneChip® confirmed the absence of a statistically significant modulation between cells exponentially growing in ethanol and glucose, although *GVP36* was called "present" in both growth conditions (data not shown).

As far as the pattern of Gvp36 expression during the shift-up is concerned, it is worth recalling that *GVP36* has been identified by ChIP-ChIP analysis as a target of Tos8, a transcription

factor that is itself a target of SBF (Swi4-Swi6 cell cycle box binding factor) (58). Nearly 20% of Tos8 target genes are devoted to some aspect of polarized growth, including several genes important for bud site selection and bud emergence. These data suggest that *GVP36* mRNA could be specifically induced during G_1 to S phase progression by SBF through Tos8, as discussed previously: during the ethanol to glucose shift-up, the drop in budding index results in the enrichment of G_1 cells in the population that is likely to account, at least partially, for the observed increase in the level of Gvp36.

Our data suggest that Gvp36 may be involved in adaptation to changes in nutrient concentration, such as nutritional shift-up and exhaustion of either nitrogen or carbon source. In fact: (i) Gvp36 transiently increases during a nutritional shift-up; (ii) *gvp36*Δ grows slower in both glucose- and glycerol-supplemented media and grows very poorly, if at all, in ethanol-supplemented media; (iii) in glucose-supplemented medium cells of the *gvp36*Δ mutant are smaller than wild type; (iv) during a nutritional shift-up from glycerol to glucose, the *gvp36*Δ mutant adapts defectively to the new carbon source; (v) the *gvp36*Δ mutant shows a defective entrance into stationary phase upon nitrogen or carbon exhaustion. These results are in keeping with information derived from systematic, genome-wide analyses that showed that *GVP36* deletion results in growth defect after germination, *i.e.* in a phase where spores need to adapt to novel nutrient conditions (59) and increased sensitivity (60) to rapamycin, a drug that inhibits the TOR pathway and whose effect is to mimic nutrient starvation (61). A further link between Gvp36 and nutrients availability is that Nup60, a subunit of the nuclear pore complex that interacts with *GVP36* open reading frame (62), is transcriptionally induced by addition of glucose and by Ras2 and Gpa2 overproduction, which are both involved in sugar sensing (63, 64), suggesting that Gvp36 could respond to the glucose sensing pathway(s) (65). Association of genes with nuclear pore complex and nuclear transport factors has, in fact, been implicated in transcriptional regulation (62).

In conclusion, data presented in this paper strongly support the notion that Gvp36 represents a novel BAR-containing protein that plays a role in vesicular traffic, in particular in endocytosis and vacuolar biogenesis, as well as being involved in actin organization. Vesicular traffic and actin cytoskeleton are both involved in polarized growth and vesicular transport is required for bud growth. The defects of *gvp36*Δ cells in adapting to nutritional stresses (carbon or nitrogen starvation, shift-up) are similar to those of other BAR-containing proteins (37, 66). Together with the expression pattern of the *GVP36* gene (58) and gene product (this paper), these data suggest that Gvp36 is involved in nutritional modulation of cell growth and division, possibly at the level of coordination of cell wall synthesis with bud emergence, as suggested by the recently discovered interaction of Gvp36 with Knr4/Smi1, a regulatory protein implicated in cell wall synthesis and bud formation (67, 68) in a complex comprising Act1 (cell wall organization, cell polarity, etc); Slt2 (cell wall organization and biogenesis); Bud6 (cell polarity and bud emergence); Cin8 (mitotic spindle organization and cell polarity); Jnm1 (mitotic spindle organization and cell polarity); Asc1 (protein involved in translation regulation); Ubc1 (protein ubiquitination); Hsp90 (chaperone cofactor-dependent protein folding); Pil1 (process unknown, protein kinase inhibitor) (67).

Acknowledgments—We thank Marzia Galli Kienle for support and critical discussion, Valeria Mapelli for help with two-dimensional PAGE and Neil Campbell for language checking of the manuscript.

REFERENCES

1. DeRisi, J. L., Iyer, V. R., and Brown, P. O. (1997) *Science* **278,** 680–686
2. Brown, A. J., Planta, R. J., Restuhadi, F., Bailey, D. A., Butler, P. R., Cadahia, J. L., Cerdan, M. E., De Jonge, M., Gardner, D. C., Gent, M. E., Hayes, A., Kolen, C. P., Lombardia, L. J., Murad, A. M., Oliver, R. A., Sefton, M., Thevelein, J. M., Tournu, H., van Delft, Y. J., Verbart, D. J., Winderickx, J., and Oliver, S. G. (2001) *EMBO J.* **20,** 3177–3186
3. Yin, Z., Wilson, S., Hauser, N. C., Tournu, H., Hoheisel, J. D., and Brown, A. J. (2003) *Mol. Microbiol.* **48,** 713–724
4. Warner, J. R. (1989) *Microbiol. Rev.* **53,** 256–271
5. Boles, E., and Zimmermann, F. K. (1993) *Arch. Microbiol.* **160,** 324–328
6. Gancedo, J. M. (1998) *Microbiol. Mol. Biol. Rev.* **62,** 334–361
7. Johnston, M. (1999) *Trends Genet.* **15,** 29–33
8. Ozcan, S., and Johnston, M. (1999) *Microbiol. Mol. Biol. Rev.* **63,** 554–569
9. Lombardo, A., Cereghino, G. P., and Scheffler, I. E. (1992) *Mol. Cell. Biol.* **12,** 2941–2948
10. Mercado, J. J., Smith, R., Sagliocco, F. A., Brown, A. J., and Gancedo, J. M. (1994) *Eur. J. Biochem.* **224,** 473–481
11. Surosky, R. T., Strich, R., and Esposito, R. E. (1994) *Mol. Cell. Biol.* **14,** 3446–3458
12. Cereghino, G. P., and Scheffler, I. E. (1996) *EMBO J.* **15,** 363–374
13. Futcher, B., Latter, G. I., Monardo, P., McLaughlin, C. S., and Garrels, J. I. (1999) *Mol. Cell. Biol.* **19,** 7357–7368
14. Griffin, T. J., Gygi, S. P., Ideker, T., Rist, B., Eng, J., Hood, L., and Aebersold, R. (2002) *Mol. Cell Proteomics* **1,** 323–333
15. Winderickx, J., Holsbeeks, I., Lagatie, O., Giots, F., Thevelein, J. M., and de Winde, H. (2003) *Yeast Stress Responses, Topics in Current Genetics*, pp. 307–386, Springer-Verlag, Berlin
16. Johnston, M., and Carlson, M. (1992) *The Molecular Biology of the Yeast Saccharomyces*, Cold Spring Harbor Laboratory, Cold Spring Harbor, NY
17. Entian, K. D., and Schuller, H. J. (1997) in *Yeast Sugar Metabolism: Biochemistry, Genetics, Biotechnology and Applications*, pp. 409–434, Technomic Publishing Co., Lancaster, Basel
18. Boucherie, H. (1985) *J. Bacteriol.* **161,** 385–392
19. Bataille, N., Thoraval, D., and Boucherie, H. (1988) *Electrophoresis* **9,** 774–780
20. Bataille, N., Regnacq, M., and Boucherie, H. (1991) *Yeast* **7,** 367–378
21. Haurie, V., Sagliocco, F., and Boucherie, H. (2004) *Proteomics* **4,** 364–373
22. Kief, D. R., and Warner, J. R. (1981) *Mol. Cell. Biol.* **1,** 1007–1015
23. Alberghina, L., Smeraldi, C., Ranzi, B. M., and Porro, D. (1998) *J. Bacteriol.* **180,** 3864–3872
24. Sturani, E., Costantini, M. G., Zippel, R., and Alberghina, F. A. (1976) *Exp. Cell Res.* **99,** 245–252
25. Alberghina, L., Rossi, R. L., Porro, D., and Vanoni, M. (2005) *Systems Biology: Definitions and Perspectives, Topics in Current Genetics*, Vol. 13, pp. 325–347, Spring-Verlag, Berlin
26. Alberghina, L., Rossi, R. L., Querin, L., Wanke, V., and Vanoni, M. (2004) *J. Cell Biol.* **167,** 433–443
27. Ghaemmaghami, S., Huh, W. K., Bower, K., Howson, R. W., Belle, A., Dephoure, N., O'Shea, E. K., and Weissman, J. S. (2003) *Nature* **425,** 737–741
28. Blader, I. J., Cope, M. J., Jackson, T. R., Profit, A. A., Greenwood, A. F., Drubin, D. G., Prestwich, G. D., and Theibert, A. B. (1999) *Mol. Biol. Cell* **10,** 581–596
29. Rabilloud, T., Strub, J. M., Luche, S., van Dorsselaer, A., and Lunardi, J. (2001) *Proteomics* **1,** 699–704
30. Fraering, P. C., Ye, W., Strub, J. M., Dolios, G., LaVoie, M. J., Ostaszewski, B. L., van Dorsselaer, A., Wang, R., Selkoe, D. J., and Wolfe, M. S. (2004)

Biochemistry **43,** 9774–9789
31. Perkins, D. N., Pappin, D. J., Creasy, D. M., and Cottrell, J. S. (1999) *Electrophoresis* **20,** 3551–3567
32. Gygi, S. P., Rochon, Y., Franza, B. R., and Aebersold, R. (1999) *Mol. Cell. Biol.* **19,** 1720–1730
33. Inadome, H., Noda, Y., Adachi, H., and Yoda, K. (2005) *Mol. Cell. Biol.* **25,** 7696–7710
34. Kumar, A., Agarwal, S., Heyman, J. A., Matson, S., Heidtman, M., Piccirillo, S., Umansky, L., Drawid, A., Jansen, R., Liu, Y., Cheung, K. H., Miller, P., Gerstein, M., Roeder, G. S., and Snyder, M. (2002) *Genes Dev.* **16,** 707–719
35. Marston, A. L., Tham, W. H., Shah, H., and Amon, A. (2004) *Science* **303,** 1367–1370
36. Peter, B. J., Kent, H. M., Mills, I. G., Vallis, Y., Butler, P. J., Evans, P. R., and McMahon, H. T. (2004) *Science* **303,** 495–499
37. Ren, G., Vajjhala, P., Lee, J. S., Winsor, B., and Munn, A. L. (2006) *Microbiol. Mol. Biol. Rev.* **70,** 37–120
38. Habermann, B. (2004) *EMBO Rep.* **5,** 250–255
39. Gavin, A. C., Aloy, P., Grandi, P., Krause, R., Boesche, M., Marzioch, M., Rau, C., Jensen, L. J., Bastuck, S., Dumpelfeld, B., Edelmann, A., Heurtier, M. A., Hoffman, V., Hoefert, C., Klein, K., Hudak, M., Michon, A. M., Schelder, M., Schirle, M., Remor, M., Rudi, T., Hooper, S., Bauer, A., Bouwmeester, T., Casari, G., Drewes, G., Neubauer, G., Rick, J. M., Kuster, B., Bork, P., Russell, R. B., and Superti-Furga, G. (2006) *Nature* **440,** 631–636
40. Friesen, H., Humphries, C., Ho, Y., Schub, O., Colwill, K., and Andrews, B. (2006) *Mol. Biol. Cell* **17,** 1306–1321
41. Iida, H., and Yahara, I. (1984) *J. Cell Biol.* **98,** 1185–1193
42. Vanoni, M., and Johnson, S. P. (1991) *Eur. J. Cell Biol.* **55,** 179–182
43. Kubota, S., Takeo, I., Kume, K., Kanai, M., Shitamukai, A., Mizunuma, M., Miyakawa, T., Shimoi, H., Iefuji, H., and Hirata, D. (2004) *Biosci. Biotechnol. Biochem.* **68,** 968–972
44. Munn, A. L., Stevenson, B. J., Geli, M. I., and Riezman, H. (1995) *Mol. Biol. Cell* **6,** 1721–1742
45. Brizzio, V., Gammie, A. E., and Rose, M. D. (1998) *J. Cell Biol.* **141,** 567–584
46. Mulholland, J., Wesp, A., Riezman, H., and Botstein, D. (1997) *Mol. Biol. Cell* **8,** 1481–1499
47. Moseley, J. B., and Goode, B. L. (2006) *Microbiol. Mol. Biol. Rev.* **70,** 605–645
48. Belmont, L. D., and Drubin, D. G. (1998) *J. Cell Biol.* **142,** 1289–1299
49. Ayscough, K. R., Stryker, J., Pokala, N., Sanders, M., Crews, P., and Drubin, D. G. (1997) *J. Cell Biol.* **137,** 399–416
50. Zheng, B., Wu, J. N., Schober, W., Lewis, D. E., and Vida, T. (1998) *Proc. Natl. Acad. Sci. U. S. A.* **95,** 11721–11726
51. Vida, T. A., and Emr, S. D. (1995) *J. Cell Biol.* **128,** 779–792
52. Goffeau, A., Barrell, B. G., Bussey, H., Davis, R. W., Dujon, B., Feldmann, H., Galibert, F., Hoheisel, J. D., Jacq, C., Johnston, M., Louis, E. J., Mewes, H. W., Murakami, Y., Philippsen, P., Tettelin, H. and Oliver, S. G. (1996) *Science* **274,** 563–567
53. Hughes, T. R., Robinson, M. D., Mitsakakis, N., and Johnston, M. (2004) *Curr. Opin. Microbiol.* **7,** 546–554
54. Roberts, G. G., and Hudson, A. P. (2006) *Mol. Genet. Genomics* **276,** 170–186
55. Chowdhury, S., Smith, K. W., and Gustin, M. C. (1992) *J. Cell Biol.* **118,** 561–571
56. Bowers, K., and Stevens, T. H. (2005) *Biochim. Biophys. Acta* **1744,** 438–454
57. Care, A., Vousden, K. A., Binley, K. M., Radcliffe, P., Trevethick, J., Mannazzu, I., and Sudbery, P. E. (2004) *Genetics* **166,** 707–719
58. Horak, C. E., Luscombe, N. M., Qian, J., Bertone, P., Piccirrillo, S., Gerstein, M., and Snyder, M. (2002) *Genes Dev.* **16,** 3017–3033
59. Deutschbauer, A. M., Williams, R. M., Chu, A. M., and Davis, R. W. (2002) *Proc. Natl. Acad. Sci. U. S. A.* **99,** 15530–15535
60. Xie, M. W., Jin, F., Hwang, H., Hwang, S., Anand, V., Duncan, M. C., and Huang, J. (2005) *Proc. Natl. Acad. Sci. U. S. A.* **102,** 7215–7220
61. Crespo, J. L., and Hall, M. N. (2002) *Microbiol. Mol. Biol. Rev.* **66,** 579–591
62. Casolari, J. M., Brown, C. R., Komili, S., West, J., Hieronymus, H., and Silver, P. A. (2004) *Cell* **117,** 427–439
63. Rolland, F., Winderickx, J., and Thevelein, J. M. (2002) *FEMS Yeast Res.* **2,** 183–201
64. Thevelein, J. M., and de Winde, J. H. (1999) *Mol. Microbiol.* **33,** 904–918
65. Wang, Y., Pierce, M., Schneper, L., Guldal, C. G., Zhang, X., Tavazoie, S., and Broach, J. R. (2004) *PLoS Biol.* **2,** E128
66. Bauer, F., Urdaci, M., Aigle, M., and Crouzet, M. (1993) *Mol. Cell. Biol.* **13,** 5070–5084
67. Basmaji, F., Martin-Yken, H., Durand, F., Dagkessamanskaia, A., Pichereaux, C., Rossignol, M., and Francois, J. (2006) *Mol. Genet. Genomics* **275,** 217–230
68. Martin-Yken, H., Dagkessamanskaia, A., Talibi, D., and Francois, J. (2002) *Curr. Genet.* **41,** 323–332

Proteomic Analysis of a Nutritional Shift-up in *Saccharomyces cerevisiae* Identifies Gvp36 as a BAR-containing Protein Involved in Vesicular Traffic and Nutritional Adaptation

Lorenzo Querin, Rossella Sanvito, Fulvio Magni, Stefano Busti, Alain Van Dorsselaer, Lilia Alberghina and Marco Vanoni

J. Biol. Chem. 2008, 283:4730-4743.
doi: 10.1074/jbc.M707787200 originally published online December 21, 2007
